RESEARCH

Open Access

Effect of nano-fluorapatite filler particles on surface microhardness and mineralization capacity of an experimental oral film

Dalia Y. Zaki[1], Engie M. Safwat[1], Haidy N. Salem[1*], Shaymaa M. Nagi[1], Tamer M. Hamdy[1], Lamiaa M. Moharam[1], Mohammad L. Hassan[2] and Marwa A. Sherief[3]

Abstract

Background The objective of the study was to prepare and assess novel remineralizing oral films loaded with fluorapatite powder and composed of a combination of hydroxyethyl cellulose (HC) and cellulose nanofibers (CF).

Methods Three concentrations of the prepared nano-fluorapatite were tried and tested after loading in the cellulose blends and films were prepared using solvent cast technique. Along with SEM, measurements of thickness of film, bending tolerance, time of disintegration, surface pH and release of ions were made. The produced film's ability to remineralize demineralized teeth in vitro was investigated.

Results The findings showed that the films' thicknesses were uniform, their folding endurance exceeded 300, and their disintegration times exceeded 24 h. High amounts of fluoride and calcium ions were released, and nearly neutral pH values were observed. The distribution of fluorapatite powder particles was uniform, as demonstrated by SEM. The Vickers microhardness (VHN) of enamel and morphological analysis results showed that in comparison with the demineralized specimens, there was a substantial microhardness value increase following 15 and 30 days remineralization.

Conclusions Newly developed prepared films are a successful method for remineralizing early-stage demineralized tooth lesions.

Keywords Oral films, Remineralizing, Fluorapatite, Microhardness

Background

The goals of prevention of initial dental caries are to maintain physiological balance and stop the caries before it starts. Conversely, secondary prevention entails early

*Correspondence:
Haidy N. Salem
haidy_salem@hotmail.com
[1] Restorative and Dental Materials Department, National Research Center, Dokki, Giza, Egypt
[2] Cellulose and Paper Department, Centre of Excellence for Advanced Sciences, National Research Centre, Giza, Egypt
[3] Inorganic Chemistry Department, National Research Center, Dokki, Giza, Egypt

detection and intervention through non-operative treatment to stop the advancement of the disease. (Gala et al. 2019, Zaki and Hamzawy 2018).

Remineralization of enamel is the process of precipitation of mineral phases in between the crystals and rods gaps, or the partial minerals substitution in enamel and dentin from the surrounding environment. While fluoride is a crucial active component in treatments intended for remineralization on the market today, minerals like phosphate and calcium are required for remineralization (Abdelnabi et al. 2020).

As a result, novel remineralization compositions have been studied to augment the fluoride impact and to

supply calcium and phosphate continuously in the vicinity of caries lesions. There are commercial products that contain the remineralizing agents (bioactive glass and tricalcium phosphate (T-C-P) in the form of chewing gums, tooth pastes, varnishes or gels. These products do, however, have a brief duration of action that is restricted to the application period. (Anil et al. 2022).

Oral thin films OTFs are intraoral flat films used to deliver systemically active component for drugs over the counter. These films may contain pharmacological compounds in the form of soluble, insoluble or taste-masked compounds. The right kinds of polymers could be selected to create qualities that are specifically tuned to meet API loading requirements and disintegrating rates. (Pedram et al. 2023; Gandhi et al. 2021).

Numerous medications can be carried by cellulose nanofibers (CF), which can create a 3D film with great porosity. CF has undergone experimental testing in the form of oral films as a medication carrier. Researchers assessed the medications' capacity to permeate through oral films made of cellulose nanofibers while they were in solution. Because CF is a natural, safe, and biodegradable polymer, scientists have been inspired to create mucoadhesive mineral-releasing films and CF to treat local dental conditions including periodontitis conditions (Alopaeus et al. 2020).

Conversely, some research have investigated oral films containing hydroxyethyl cellulose (HC), one of the widely utilized derivatives of cellulose. In contrast to other oral films that are mucoadhesive, HC oral films had the efficient muco-adhesion to enhance the standard treatment of oral diseases.

To the greatest extent of our knowing, limited researches have been done on the utilization of CF and/or HC as oral thin films for dental remineralization, which may participate in dental caries prevention and treatment. Owing to HC's water solubility, films manufactured from it are sensitive to aqueous media, which can cause deformation and the film to lose essential mechanical qualities. CF could be used in HC film as a reinforcing matrix to get over this problem. (Abouhussein et al. 2020).

The current study's goal was to formulate a novel oral film that would prevent and treat initial dental caries by loading a bioactive nano-fluorapatite powder in a HC/CF nanocomposite film. The produced films were tested in vitro for their ability to release calcium, phosphorus, and fluoride continuously over the course of 12 hours, which might be employed as a remineralizing agent when oral fluids came into contact with them.

Methods

A bleached sugar cane bagasse pulp for Pulp and Paper was used to prepare TEtra-Methyl-Piperidine-Oxoammonium (TEMPO)-oxidized cellulose nanofibers. The chemical composition of bagasse pulp and reagent-grade chemicals are shown in Table 1.

Cellulose nanofibers preparation

Three grams of bleached bagasse pulp were mixed with 0.048 g, 0.3 mmol from TEtra-Methyl-Piperidine-Oxoammonium salt and 0.48 g, 4.8 mmol from sodium bromide in 400 milliliters of distilled water. Next, in order to pH to 10, 30 milliliters of solution from sodium

Table 1 Materials and their manufacturers used in this study

	Chemicals	Manufacturers
1	Bagasse pulp 70.6% alpha-cellulose, 26.8% pentosans, 0.82% ash	Qena Comp
2	Sodium hypochlorite	(Adwic, Egypt)
3	Sodium chlorite	(Adwic, Egypt)
4	TEtra-Methyl-Piperidine-Oxoammonium salt TEMPO	Sigma-Aldrich, USA
5	Na-OH Sodium hydroxide	Modern laboratory-Egypt
6	Alcohol (Ethanol)	Adwic- Egypt
7	Na-Br Sodium Bromide	Sigma-Aldrich-USA
8	HC Hydroxyethyl cellulose	Sigma-Aldrich, USA,
10	Ammonium dihydrogen phosphate	Hayashi Pure Chemical, Japan
11	Lactic acid, Calcium nitrate, Potassium chloride	Alfa Aesar-UK
14	Ca- carbonate	SRL-India
15	Na- carbonate	Adwic- Egypt
16	Ca- fluoride	BDH- UK
17	Tris buffer	Sigma-Aldrich, USA
18	Silica sand	Western Desert, Egypt

hypochlorite was mixed with the solution. At the end, ethanol was added, and pH was observed until reaching 7. Next, the fibers were refined by repeatedly water rinsing and centrifuging them at a speed of 10,000 revolutions per minute using a centrifuge machine by Sigma-Laborzentrifugen-GmbH, Germany. Lastly, dialysis against distilled water was performed by dialysis machine (3500MWCO Spectra/Pro) to refine the oxidized cellulose nanofibers for a week while changing the water. After being thinned out using water to a 2 % consistency, the purified oxidized fibers were then homogenized at 20,000 rpm speed using a homogenization machine (M-Zipperer GmbH-Germany).

Cellulose nanofibers characterization

The characterization was performed by FTIR Fourier transform infrared spectroscopy (FTIR -6800-JASCO, USA). By using an acid-base titration technique created for conductometric titrations via a conductometer (Jenway- 7200-UK), the quantity of carboxylic groups was verified. The 50 mg nanofibers were stirred constantly while being suspended in 15 milliliters of (HCl) hydrochloric acid solutions. Next, 0.01 milliliters of (NaOH) sodium hydroxide solution was used to titrate the suspensions that were produced. The oxidized nanofibers had a carboxylic content of 0.64 mol/g.

Next, the analysis was performed using a transmission electron microscope (JEOL-1230 -Japan)

Nano-fluorapatite powder preparation

As Ca and P-precursors, calcium nitrate tetrahydrate (Ca-(NO3)2·4H2O, Merck, GR) and diammonium hydrogen phosphate (Aldrich, USA) were selected. Ammonium fluoride (NH4F Merck) is a source of F, and urea (CH4N2O Aldrich, USA) was used as gelling and ammonium donor agent. EDTA (C10H16N2O8 Aldrich, USA) was used as chelating calcium ions in the course of gel formation by using ammonia solution. Ammonia solution was heated at 60 °C, and then 181 g EDTA was added while stirring until complete dissolution. Aqueous solution (200 ml) of 129 g calcium nitrate tetrahydrate, diammonium hydrogen phosphate (39.83 g), ammonium fluoride (15 g) and urea (40.20 g) were then mixed to the prepared solution. The prepared mix was then heated at 100 °C for 4 h. The obtained gel was dried at 350 °C under ambient static air.

Characterization of nano-fluorapatite-based powder

Thirty milligram (30 mg) powdered sample was heated at a rate of 10 °C per minute using Shimadzu DTG-60H, Shimadzu, Japan, differential thermo-analysis (DTA) analyzer. After heat treatment, the produced phases were recognized by Cu Kα radiation-based XRD X-ray powder diffraction (MiniFlex-Rigaku-Japan).

Preparation of oral films (HC/CF)

95% of hydroxyethyl cellulose (HC) and 5% of cellulose nanofibers (CF) were blended, and solvent casting technique was used for films preparation. The blends were cast in glass Petri plates 12 cm in diameter. Dry weight of CF (2.4g) was dispersed in 1200 ml of water to produce CF suspension (0.2%w/v) for the film manufacturing. Then, using a magnetic stirrer, 48 grams of HC hydroxyethyl cellulose powder was mixed with the CF mixture until complete dissolution.

The HC/CF suspension was then loaded with nano-fluorapatite FAp powder with the following amounts (0.1, 0.3 and 0.5 gram) to 60 milliliters of the HC/CF mix, and then the mixture was continuously stirred for 30 min at speed 500 rpm. An ultrasonic processor (Hielscher -GmbH- Germany) was used to apply 400 Watts for 5 min at a 75% amplitude. The HC/CF FAp suspensions were subsequently poured as a film in 120-mm-diameter glass petri dishes. Next, it is kept for 12 h in a furnace at 50 °C. The unloaded HC/CF films (as a control group) were cast as well. Five 120-mm-diameter films were produced ($n = 5$ for each group). Once the films had dried, they were removed by pealing from the dishes and cut into slices (2×2 cm^2 squares films). This raises the overall numbers of specimens into 240 after discarding the damaged films. Films were stored in aluminum foil for testing. The number of films, compositions, and formulation code are listed in Table 2.

Assessment of the prepared films in vitro
Visual inspection

According to Alyami et al. 2023, the prepared thin films' homogeneity, clarity, and lack of flaws or air bubbles were investigated, and appropriate qualities for films to be utilized for additional assessment were verified appropriate qualities for films to be utilized for additional assessment.

Table 2 Number of films, compositions and formulation code

Formulation code	Nano-Fluorapatite powder amount (gram)	Films numbers (2×2 cm^2)/group
HC/CF/0.1BF	0.1	60
HC/CF/0.3BF	0.3	60
HC/CF/0.5BF	0.5	60
Control = HC/CF	–	60
Total number of oral films		240

Testing of film thickness

For film thickness measurement, a calibrated digital caliper was used at three randomly selected points. The thickness mean values was then estimated. Three samples from each formulation were averaged, and the results were computed (Cua et al. 2022).

Bending endurance

The bending endurance was done by manual folding three 2×2 cm^2 film samples from each formulation in the same location until the film broke or a visible crack appeared. The bending endurance value was determined by counting the folds of the film before it broke or showed any signs of cracking (Gandhi et al. 2021). For every formulation, three film specimens have been assessed and the mean value was obtained.

Films disintegration time detection

Each film specimen was placed on the surface of a Petri plate containing 20 ml buffer solution (pH = 6.8), and disintegration times were visually determined. The period of time the film took to dissolve was calculated (Gandhi et al. 2021).

For every formulation, three film specimens were examined, and the average time was determined.

Evaluation of films surface pH

Each film specimen was treated by 0.5 ml of distilled water little by little for 30 seconds. By contacting the film with the pH meter electrode (Jenway- 3505-UK) and allowing it to settle in for one minute, the pH was determined (Köse et al. 2022).

SEM analysis

Screening was done to assess how evenly the bioactive powder were evenly distributed in the tested films by SEM- model-XL30 Philips-Netherlands.

FTIR Fourier transform infrared spectroscopy

Using a FTIR spectrometer (JASCO -6800-USA), FTIR analysis was performed to examine powder–polymer interactions (Adepu and Ramakrishna 2021). For testing, films with the greatest powder loading concentration were chosen.

Ions release testing

By embedding each film separately in buffer solution of phosphate (20 ml, pH = 6.8) and constantly circulating inside a glass container at 37 ± 0.5 °C for 50 rpm, the ions discharged from the films were assessed. Using induced-coupled-plasma spectrometer (Jobin-Yvon -Ultima 2 ICP-France), the aliquot was removed after a 12-hour immersion period, filtered through a 0.2-micron membrane, and examined to identify the released ions such as fluoride, calcium and phosphorus, ions (Pimentel et al. 2022).

Optical qualities assessment

Using an optical spectrometer (Shimadzu, Japan), the visible light transmission was measured in order to assess their optical qualities.

Assessment of the remineralization

Preparation of teeth specimens   Maxillary central incisors from bovine teeth were used. To remove any contaminants from the tooth surface, teeth were cleansed. After that, the teeth were kept for a maximum of one month at $4\,^0$C in a buffer solution (pH=7)

Preparation of enamel specimens

A low-speed hand piece with diamond disk (Edental Golden-Switzerland) was used to section central incisors roots at the cemento-enamel line. After removing the pulpal materials with an endodontic file, wax was used to seal the root canal apertures. Every part of the crown was set into an acrylic resin mold. Prior to testing, the produced specimens were stored for a full day at 37 °C in artificial saliva. Vickers hardness tester VHN was used to conduct baseline microhardness testing. (NEXUS 4000, Netherlands).

Induction of initial caries lesion

The demineralization protocol of enamel included subjecting the teeth to a pH cycling regimen including three hours of alternating demineralization in a demineralizing solution 40 ml (calcium chloride 2.2 mM, sodium dihydrogen phosphate 2.2 mM, lactic acid 0.05 mM and sodium hydroxide 5% was used to adjust the pH to reach 4.5) and in artificial saliva for remineralization (the artificial saliva: calcium nitrate tetrahydrate 1.5 mM, sodium phosphate monobasic dihydrate 0.9 mM, potassium chloride 150 mM, Tris buffer 0.1 mM, and calcium fluoride 0.03 ppm at pH = 0.57). The cycling pH protocol was adhered to five days in a row (O'Hagan-Wong et al. 2022).

Oral thin film application

After contacting demineralized labial enamel tooth surface, the film was submerged in 30 milliliters of artificial saliva for 12 h at 37 °C in a tightly sealed container. Following a 12-h period, the specimens were again submerged in 30 milliliters of new artificial saliva after being cleaned under running water. For thirty days, this cycle of remineralization was repeated. The artificial saliva was replaced every 12 h.

Zaki *et al. Bulletin of the National Research Centre*   (2024) 48:81

Page 5 of 11

Hardness VHN testing

With a Vickers hardness test VHN (NEXUS-4000, Netherlands), surface hardness was tested (a load of 200 g, a 15-s dwell time and a 20X magnification) (Mehta and Siddaiah 2022).

SEM analysis

Scanning electron microscope was used to study ultramorphological changes for the following: sound enamel, demineralized enamel, and after treatment enamel surfaces with the remineralizing thin film. The test was done for 15 and 30 days at a X8000 magnification and 30 kV excitation voltage.

Results

Cellulose nanofibers characterization TEMPO

Figure 1A photograph demonstrates the 4-5 nm width of the TEMPO-oxidized cellulose nanofibers. The isolated nanofibers' FTIR spectra are showed in Fig. 1B, which displays the typical peaks of cellulose: a stretching vibration peak O–H at 3400 cm^{-1}, a stretching vibration peak of groups CH and CH_2 at 2900 cm^{-1}, an adsorbed water peak at 1640 cm^{-1}, bending vibration peaks of CH_2 and OH groups at 1430 cm^{-1}, 1372 cm^{-1}, and 1330 cm^{-1}, stretching vibration peaks of C–O for glycosidic bonds, C–O of primary and secondary hydroxyl groups, and 1050 cm^{-1}, 1100 cm^{-1}, and 1150 cm^{-1}, and out-of-plane deformational vibration of O–H groups peak at 897 cm^{-1}. The spectra also revealed a signal at 1735 cm^{-1} attributed to the carbonyl group of the carboxylic groups,
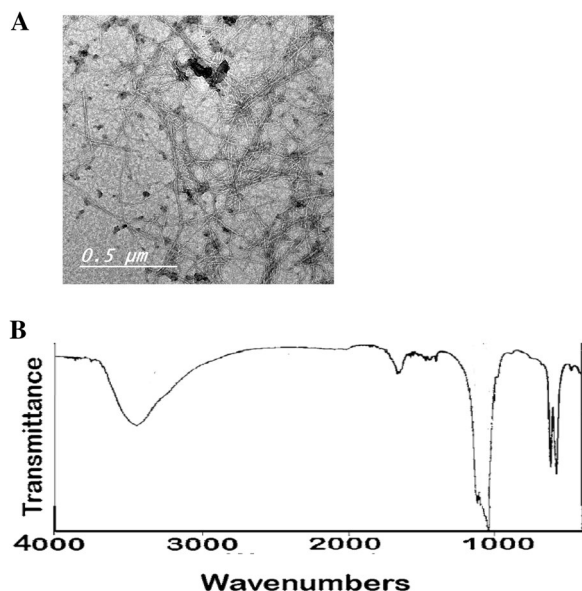

Fig. 1 **A** TEM image of oxidized cellulose nanofibers. **B** FTIR image of oxidized cellulose nanofibers

which resulted from the oxidation of cellulose. Moreover, a shift to 3430 cm^{-1} was noticed in O–H stretching vibration due to adding carboxylic acid hydroxyl groups.

Nano-fluorapatite powder characterization
XRD analysis

The XRD pattern of the prepared nano-fluorapatite-based powder is shown in Fig. 2A.

SEM analysis

SEM image of the powder with 80,000X magnification is shown in Fig. 2B.

FTIR analysis

Phosphate (PO_4^{3-}) bands are visible in the fluorapatite at 590(v4), 605(v4), 980(v4), and 1020–1095(v3) Cm-1. Hydroxyl (OH) bands are visible at 632 and 3540 Cm-1. Additionally, carbonate $(CO_3 2-)$ bands have been identified at 1660 and 1370 cm^{-1}. The fluoride ion penetration through the network of apatite is shown by a tiny peak corresponding to the bond OH-F, which exists between 3536 and 3545 cm^{-1}. Fig. 3

TEM analysis

TEM image of the prepared powder is shown in Fig. 4. Less than 100-nm-sized irregularly shaped rod and spherical particles are visible in the TEM picture.

Characterization of HC/CF/FAp films

SEM analysis   A scanning electron microscope inspection of the films was performed and are displayed in Fig. 5A and B.

Physical characterization of the prepared film   Table 3 displays the physical evaluation parameters of HC/CF/FAp films.

Upon visual inspection, the films were homogeneous and clear, lacking flaws or bubbles of air.

Film thickness, the average as well as the standard deviation (SD) of the film thicknesses in Table 3 indicated that the films' thickness increased as the loading of bioactive fluorapatite did, while the addition of CF had no discernible effect on the thickness of the HC films. The homogeneity of the thickness created by the fabrication process is indicated by the low standard deviation (SD) values of the film thickness (Fig. 6 A and B).

The folding endurance of the tested films was found to be greater than 300, as indicated by Table 3's results.

Surface pH, the produced films' mean ± standard deviation of pH values was determined and recorded in Table 3. The fluorapatite-filled films' surface pH ranged from 6.3 to 6.63 pH.
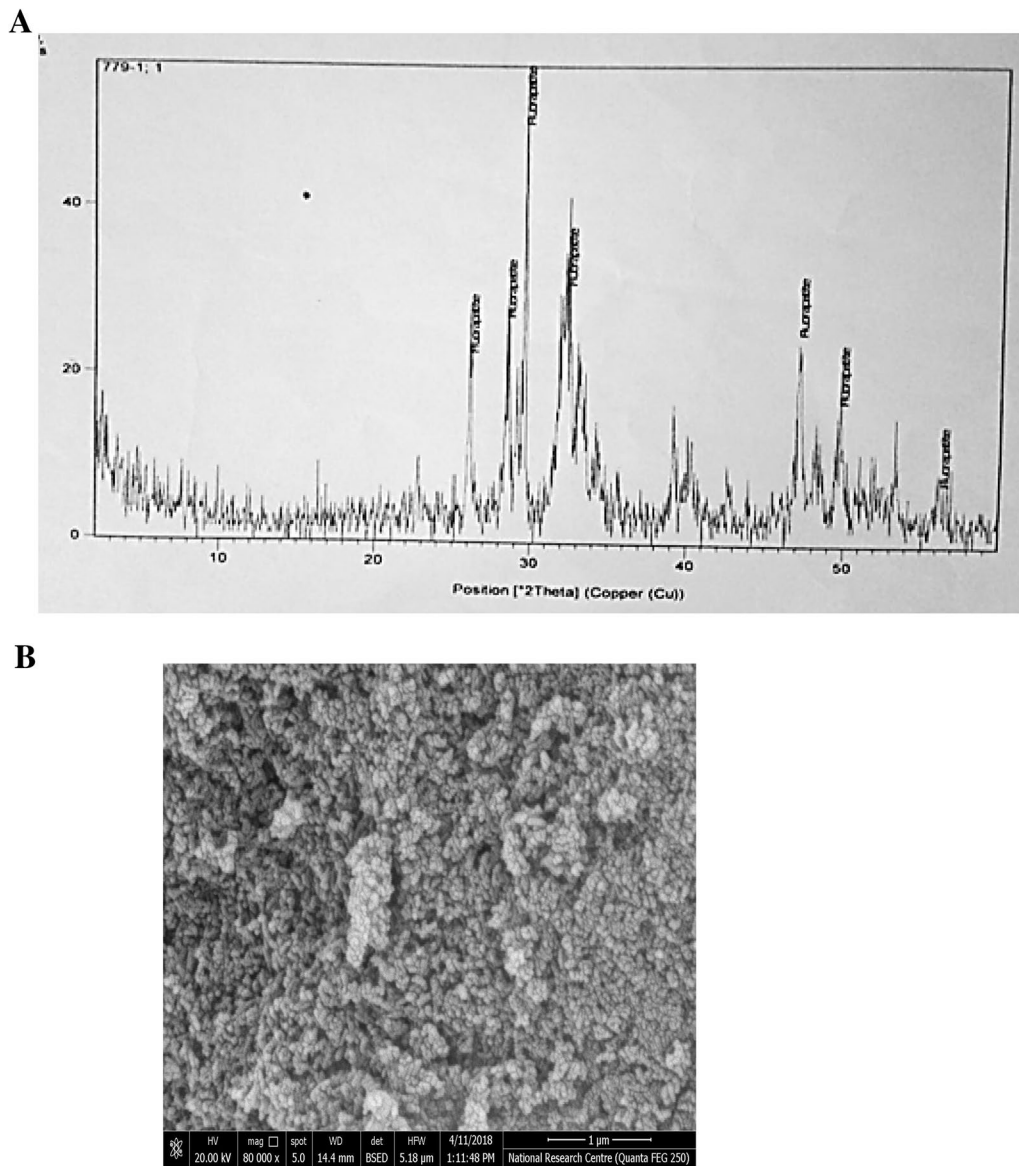
A

B

Fig. 2 **A** XRD pattern for nano-fluorapatite powder. **B** SEM micrograph for nano-fluorapatite powder

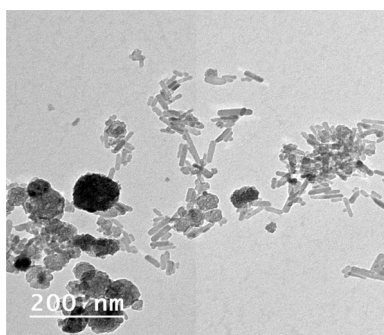**Fig. 3** FTIR spectra of 0.5 gm nano-fluorapatite loaded film

Zaki *et al. Bulletin of the National Research Centre*   (2024) 48:81

Page 7 of 11

Fig. 4 Transmission electron microscopy TEM shows nanoparticles with rod and spherical irregular shaped particles
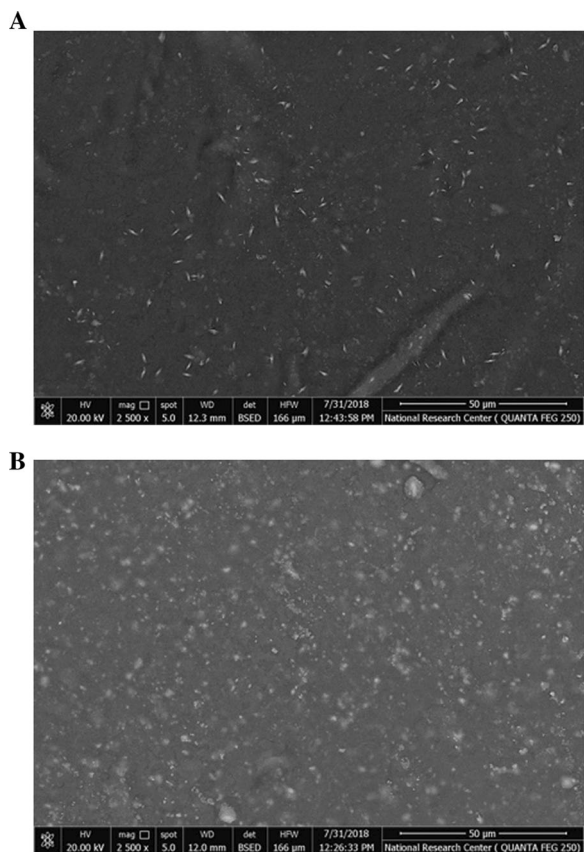
Table 3 Physical evaluation parameters of HC/CF/FAp films

Formulation code	Thickness (mm)	Folding endurance (No. of folds)	Surface pH	Disintegration time
HC	0.134±0.002	> 300	8.1±0.046	42 min
HC/CF/0.1F	0.092±0.004	> 300	6.63±0.092	> 24
HC/CF/0.3F	0.0996±0.009	> 300	6.4±0.309	> 24
HC/CF/0.5F	0.0883±0.003	> 300	6.5±0.613	> 24
HC/CF	0.092±0.004	> 300	7±0.225	> 24

demonstrated the film's consistent expansion following a 24-h immersion period.

Testing of ions release

Table 4 provides the ions emitted from prepared films along with their mean and standard deviation values (ppm). The outcomes showed that significant amounts of fluoride and calcium ions were released. Significant variations in the amounts of ions released between samples were shown by statistical analysis.

Optical properties

Values for light transmission were as follows: 81.21, 79.31, 37.22, 9.31 for HC, HC/CF, HC/CF 0.1 BF, HC/CF 0.3 BF HC/CF 0.5 BF, respectively.

Assessment of the prepared film's remineralizing impact in vitro on dental cavities experimentally induced in extracted teeth

Surface hardness

There was a distinct difference in surface hardness values, after 15 and 30 days, between all specimens, according to the statistical analysis shown in Table 5. After 15 and 30 days, there was a distinct change in the hardness values; samples after 30 days testing exhibited a higher increase in hardness values.

In comparison with the demineralized specimens, the study's results showed a substantial increase in hardness values for 15 and 30 days after remineralization process for HC/CF/0.5 BF film.

SEM analysis

Figure 7 displays the tested specimens' SEM pictures. Following demineralization, the enamel displayed a maintained periphery with lost core structure. A mineral layer developed on the enamel during the 15–30 day remineralization therapy, repairing the enamel's core flaw. For 30 days, when film HC/CF/0.5 BF was used, nearly total coverage of the enamel surface occurred, and scaffolding deposits with cluster-like structures resembling
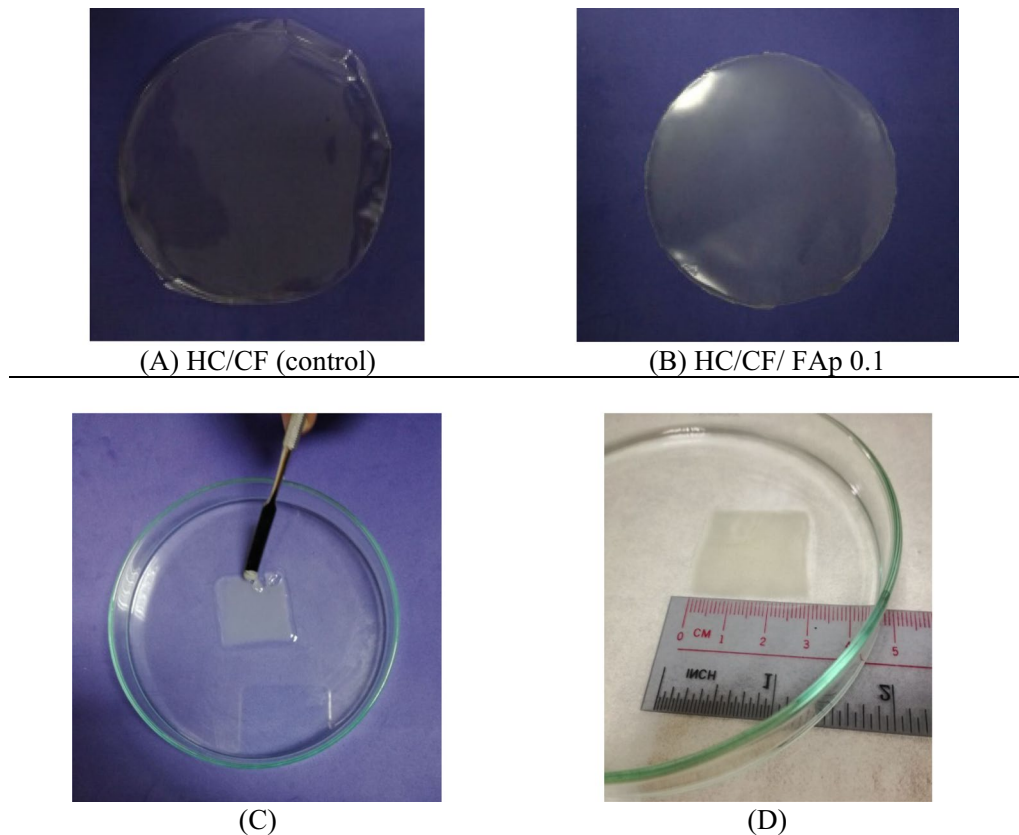

Fig. 5 A SEM micrographs of HC/CN (control film). **B** SEM micrographs of a film loaded with 0.5 gm fluorapatite powder (HC/CF/ 0.5 BF)

The disintegration time of fast-dissolving films used for medication administration is within the range of 5–57 s. After soaking in water for 24 h, the films exhibited partial dissolution and got larger in size from 2 to roughly 3 cm^2. By the end of the test, the films did not dissolve (Fig. 6C, D). The photographs also

(A) HC/CF (control)

(B) HC/CF/ FAp 0.1

(C)

(D)

Fig. 6 **A** Photographs of prepared HC/CF film (control), **B** HC/CF/ FAp 0.1. **C** and **D** Photographs of prepared HC/CF films at the end of the disintegration time

Table 4 Ions release mean and standard deviation values

Formulation code	Calcium ions	Phosphorus ions	Fluoride ions
HC/CF/0.1 BF	$262.6^c \pm 0.1$	$5820.0^c \pm 0.1$	$135.2^d \pm 0.1$
HC/CF/0.3 BF	$264.1^d \pm 0.1$	$6065.8^d \pm 0.1$	$146.1^e \pm 0.1$
HC/CF/0.5 BF	$1247.9^f \pm 0.1$	$6090.7^e \pm 0.1$	$146.4^e \pm 0.2$
Phosphate buffer solution	–	11156^g	–

Different letters indicate significance difference, * at ($p < 0.05$)

Table 5 Vickers hardness number VHN results of ANOVA test at the following: base line, after demineralization and after remineralization (for 15 and 30 days)

	Base line	After demineralization	After remineralization		p value
			15 days	30 days	
HC/CF 0.5 BF	127^c	41^a	104.8^b	131.7^c	

Different letters indicate significance difference, *: ($p < 0.05$)

the commencement of the remineralization process were clearly visible on the enamel surface (Fig. 7D).

Discussion

To demonstrate the chemical structure of cellulose nanofibers, the isolated nanofibers' FTIR spectra are showed in Fig. 1B, which displays the typical peaks of cellulose: (Li et al. 2023). The XRD pattern of the prepared nano-fluorapatite-based powder is shown in Fig. 2A. The fluorapatite $(CaF)Ca_4(PO4)_3$ (Ref.Code: 00-002-0845) chemical formula of the nanosized particles was revealed by the XRD peaks. The carbonate (CO_3^{2-}) bands have been identified at 1660 and 1370 cm^{-1}, which suggests that carbonate groups have been replaced within the apatite structure. The fluoride ion penetration through the network of apatite is shown by a tiny peak corresponding to the bond OH-F, as demonstrated by FTIR analysis Fig. 3

Less than 100-nm-sized irregularly shaped rod and spherical particles are visible in the TEM picture as shown in Fig. 4. This result is consistent with the particle size measurements made using the XRD pattern in Fig. 2A.
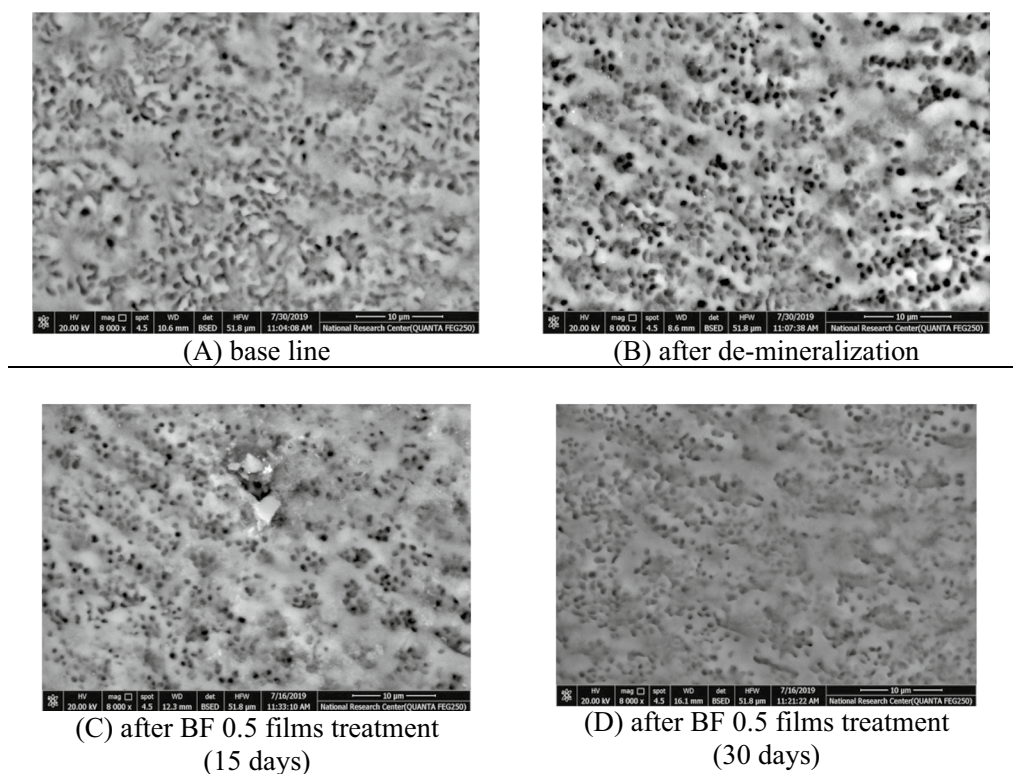
(A) base line

(B) after de-mineralization

(C) after BF 0.5 films treatment
(15 days)

(D) after BF 0.5 films treatment
(30 days)

Fig. 7 **A** SEM images for base line (sound enamel) **B** SEM images for enamel after demineralization **C** SEM images for enamel after BF 0.5 films treatment (15 days) **D** SEM images for enamel after BF 0.5 films treatment (30 days)

To prepare the oral thin films, a blend of HC and CF was utilized, with varying percentages of fluorapatite as shown in Table 2. It is very critical to take into consideration the addition of fluorapatite particles in a properly formulated medium to prevent the remineralization of white spot lesions. To ensure that the powder particles were distributed uniformly throughout the films, a SEM inspection of the films was performed and are displayed in Fig. 5A and B. The analysis demonstrated a homogenous distribution of the powder particles. In the instance of the HC/CF film, white, thin-shaped items were observed; these might be CF aggregation at the film's surface (Li et al. 2023). The results of the pilot study indicated that 12-cm diameter Petri dishes may be used to prepare films of thickness 0.1–0.15 mm. In this research, the nano-fluorapatite powder was carried on the CF thin film, which has distinctive hydrogel qualities. Its nearly neutral pH and gradual solubility made it the perfect medium for the remineralizing effect and to provide a foundation for ions discharge over time, preventing the quick washing of minerals off from the surface hence maximizing the benefits of remineralization (Tiskaya et al. 2021).

Upon visual inspection, the films were homogeneous and clear, lacking flaws or bubbles of air (Pacheco et al. 2021). The average as well as the standard deviation (SD) of the film thicknesses in Table 3 indicated that the films' thickness increased as the loading of bioactive fluorapatite did, while the addition of CF had no discernible effect on the thickness of the HC films. The homogeneity of the thickness created by the fabrication process is indicated by the low standard deviation (SD) values of the film thickness (Fig. 6A and B).

Conversely, folding endurance provides insight into the stiffness of the prepared films, ensuring that they can resist handling, processing, and packing without breaking down. The folding endurance of the tested films was found to be greater than 300, as indicated by Table 3's results. This is most likely because the manufactured films were thicker than typical oral thin films used for delivering drugs.

In order to prevent adverse effects on the oral mucosa, one crucial criterion is the surface pH of oral films. As per Pichayakorn et al. 2022, pH ought to be neutral or nearly neutral. Additional research revealed that pH should be roughly 6.8, which is the pH of the oral cavity. The produced films' mean ± standard deviation of pH values was determined and recorded in Table 3. The fluorapatite-filled films' surface pH ranged

from 6.3 to 6.63 pH, which is close to neutral and is therefore anticipated to be more patient-acceptable.

The time at which an oral thin film starts dissolving while it gets into contact with saliva or water is known as the disintegration period. The disintegration time of fast-dissolving films used for medication administration is typically within the range of 5–57 s. However, in this work, a longer disintegration time is needed for the loaded bioactive powders to dissolve and discharge ions over an extended period of time. After soaking in water for 24 h, the films exhibited partial dissolution and got larger in size from 2 to roughly 3 cm^2. By the end of the test, the films did not dissolved and maintained a satisfactory strength (Fig. 6C, D). The photographs also demonstrated the film's consistent expansion following a 24-h immersion period.

Testing for ion release (Ca^{++}, PO_4^{---}, and F^-) was conducted following a 12-h immersion period, which corresponded to the treatment's night-time length. The sample with the higher loading of FAp filler, HC/CF 0.5 BF, exhibited the most calcium and fluoride ion release.

After keeping the films in the buffer solution, there was a noticeable reduction in the release of phosphorus ions. This could probably occur due to ions saturation in the solution after precipitation of phosphorous ions. (Mocquot et al. 2020). Prior research on ions that applied topically has shown that fluorapatite forms and deposits onto or into demineralized enamel at greater concentrations of calcium, fluoride, and phosphate (Biria et al. 2021). Furthermore, fluoride concentrations in normal saliva higher than 0.03 ppm may promote remineralization in vitro while suppressing demineralization. For the purpose of controlling caries, the produced films used in this investigation may therefore be regarded appropriate.

The optical properties were assessed by using visible light spectroscopy. The expected result of CF's nanodiameter, which permitted the passage of the majority of incident light, is the extremely close light transmittance between HC and HC/CF. Light transmission decreased when fluorapatite was added to HC/CF, particularly with addition of 0.30 and 0.50 gram fluorapatite. It is possible that the fluorapatite's crystalline structure could reflect incident light and subsequently decrease in light transmittance after powder addition.

The impact of the HC/CF/0.5 BF film sample on the ultra-morphology and microhardness of demineralized enamel was assessed in this study. Since organic elements like dental bacteria or plaque were not included in this study, alterations seen on the enamel surface may be directly linked to the evaluated films' ability to remineralize. The pH and ions at the tooth surface were essential for remineralization in this case. Because bovine's enamel and human enamel are similar in terms of hardness,

density, and tensile strength, bovine enamel was utilized as a substitute. To replicate the oral cavity's minimal cariogenic challenge, 3 h were allotted for demineralization during the pH cycling phase (Pacheco et al. 2021)

The basics for remineralization and demineralization in vitro are first affected by ion release, pH and solubility of enamel. In surroundings environment, the inorganic content of the fluorapatite powder interacted to release ions: fluoride F, phosphorus (PO_4^{3-}), and calcium (Ca^{2+}). At the powder-liquid boundary, Na^+ with H^+ or H_3O^+ fast ionic exchange enables Ca^{2+} and PO_4^{3-} release and the creation of an overloaded ion reservoir for the hydroxyapatite enamel.

Furthermore, following the dissolution of the bioactive FAp powder network, silanols underwent reorganization by polycondensation, serving as nucleation sites. The combination of undissolved bioactive FAp powder particles and unbound phosphate and calcium resulted in the production of a protective calcium phosphate-loaded layer on the enamel surface. (Abbassy et al. 2021). Additionally, the particles containing fluoride produce fluorapatite over time in addition to hydroxyapatite. Fluorapatite is well known for its ability to remineralize and to increase the hardness values (Al-Eesa et al. 2021). Fluoride has an anticariogenic influence because it can form fluorapatite, which has more resistance to acid attack than hydroxyapatite. This may possibly be the reason for the increase in hardness values after 30 days of remineralization using film HC/CF/0.5 BF as opposed to the 15-day process. This result was consistent with earlier research (Aldhaian et al. 2021).

Since the adhesion to mucosa and mechanical properties of oral films are very important in their outcome, consequently further researches are required to assess these physical properties are important as well. Since oral thin films are relatively novel in the dental field, more reviews are needed to explore and analyze various techniques to assess and appraise the physical properties and adhesion of oral films.

Conclusions

It is possible to draw the conclusion, within the constraints of the present investigation, that the films made with the HC/CF mixture offer a film with physical properties that are appropriate for the use of tooth remineralization. Early demineralized tooth lesions could be successfully remineralized by loading films with fluorapatite (FAp), which effectively supplied the necessary ions. It will offer fresh approaches to conservatively treating and preventing early dental caries.

Abbreviations
HC   Hydroxyethyl cellulose
CF   Cellulose nanofibers

Zaki *et al. Bulletin of the National Research Centre*   (2024) 48:81

Page 11 of 11

T-C-P	Tri-calcium phosphate
TEMPO	TEtra-Methyl-Piperidine-Oxoammonium
Ca	Calcium
Na	Sodium
FAp	Nano-fluorapatite
SEM	Scanning electrode microscope
OTF	Oral thin films
FTIR	Fourier transform infrared
HCl	Hydro-chloric acid
NaOH	Sodium hydroxide
DTA	Differential thermo-analysis
XRD	X-ray powder diffraction

Availability of data and materials
Data are available under reasoning demand.

Declarations

Ethics approval and consent to participate
Not applicable

Consent for publication
Not applicable.

Competing interests
No competing interests.

References
Abbassy MA, Bakry AS, Almoabady EH, Almusally SM, Hassan AH (2021) Characterization of a novel enamel sealer for bioactive remineralization of white spot lesions. J Dent 109:103663

Abdelnabi A, Hamza MK, El-Borady OM, Hamdy TM (2020) Effect of different formulations and application methods of coral calcium on its remineralization ability on carious enamel. Open Access Maced J Med Sci 8:94–99

Abouhussein D, El Nabarawi MA, Shalaby SH, Abd El-Bary A (2020) Cetylpyridinium chloride chitosan blended mucoadhesive buccal films for treatment of pedi- atric oral diseases. J Drug Deliv Sci Technol 101676

Adepu S, Ramakrishna S (2021) Controlled drug delivery systems: current status and future directions. Molecules (basel, Switzerland) 26(19):5905

Aldhaian BA, Balhaddad AA, Alfaifi AA, Levon JA, Eckert GJ, Hara AT, Lippert F (2021) In vitro demineralization prevention by fluoride and silver nanoparticles when applied to sound enamel and enamel caries-like lesions of varying severities. J Dent 104:103536

Al-Eesa NA, Fernandes SD, Hill RG, Wong FSL, Jargalsaikhan U, Shahid S (2021) Remineralising fluorine containing bioactive glass composites. Dent Mater off Publ Acad Dent Mater 37(4):672–681

Alopaeus JF, Hellfritzsch M, Gutowski T, Scherließ R, Almeida A, Sarmento B, Škalko-Basnet N, Tho I (2020) Mucoadhesive buccal films based on a graft co-polymer—A mucin-retentive hydrogel scaffold. Eur J Pharm Sci off J Eur Fed Pharm Sci 142:105142

Alyami HS, Ali DK, Jarrar Q, Jaradat A, Aburass H, Mohammed AA, Alyami MH, Aodah AH, Dahmash EZ (2023) Taste masking of promethazine hydrochloride using l-arginine polyamide-based nanocapsules. Molecules (basel, Switzerland) 28(2):748

Anil A, Ibraheem WI, Meshni AA, Preethanath RS, Anil S (2022) Nano-hydroxyapatite (nHAp) in the remineralization of early dental caries: a scoping review. Int J Environ Res Public Health 19(9):5629

Biria M, Iranparvar P, Fatemi SM, Nejadian M, Eslamiamirabadi N (2021) In vitro effects of three fluoride-free pastes on remineralization of initial enamel carious lesions. Pediatr Dent 43(5):389–395

Cua J, Crespo E, Phelps S, Ramirez R, Roque-Torres G, Oyoyo U, Kwon SR (2022) Tooth color change and erosion: hydrogen peroxide versus non-peroxide whitening strips. Oper Dent 47(3):301–308

Gala RP, Morales JO, McConville JT (2019) Preface to advances in thin film technologies in drug delivery. Int J Pharm 571:118687

Gandhi NV, Deokate UA, Angadi SS (2021) Formulation, optimization and evaluation of nanoparticulate oral fast dissolving film dosage form of nitrendipine. AAPS PharmSciTech 22(6):218

Köse MD, Ungun N, Bayraktar O (2022) Eggshell membrane based turmeric extract loaded orally disintegrating films. Curr Drug Deliv 19(5):547–559

Li M, Jiang B, Cao S, Song X, Zhang Y, Huang L, Yuan Q (2023) Flexible cellulose-based piezoelectric composite membrane involving PVDF and $BaTiO_3$ synthesized with the assistance of TEMPO-oxidized cellulose nanofibrils. RSC Adv 13(15):10204–10214

Mehta DV, Siddaiah SB (2022) Evaluation of three different remineralizing agents on artificially demineralized enamel lesions: using scanning electron microscopy-energy dispersive X-ray and magic-angle spinning nuclear magnetic resonance—an in vitro study. J Indian Soc Pedod Prev Dent 40(3):330–337

Mocquot C, Attik N, Pradelle-Plasse N, Grosgogeat B, Colon P (2020) Bioactivity assessment of bioactive glasses for dental applications: a critical review. Dent Mater off Publ Acad Dent Mater 36(9):1116–1143

O'Hagan-Wong K, Enax J, Meyer F, Ganss B (2022) The use of hydroxyapatite toothpaste to prevent dental caries. Odontology 110(2):223–230

Pacheco MS, Barbieri D, da Silva CF, de Moraes MA (2021) A review on orally disintegrating films (ODFs) made from natural polymers such as pullulan, maltodextrin, starch, and others. Int J Biol Macromol 178:504–513

Pedram P, Najafi F, Heidari S, Hodjat M, Bolhari B, Hooshmand T (2023) Synthesis and characterization of a dental cement based on bioactive glass/zinc oxide modified with organic resin as a novel pulp capping agent. Biomed Mater (bristol, England). https://doi.org/10.1088/1748-605X/ace227

Pichayakorn W, Monton C, Sampaopan Y, Panrat K, Suksaeree J (2022) Fabrication and characterization of buccal film loaded self-emulsifying drug delivery system containing *Lysiphyllum strychnifolium* stem extracts. AAPS PharmSciTech 23(6):194

Pimentel de Oliveira R, de Paula BL, Ribeiro ME, Alves E, Costi HT, Silva C (2022) Evaluation of the bond strength of self-etching adhesive systems containing HEMA and 10-MDP monomers: bond strength of adhesives containing HEMA and 10-MDP. Int J Dent 2022:5756649

Tiskaya M, Gillam D, Shahid S, Hill R (2021) A potassium based fluorine containing bioactive glass for use as a desensitizing toothpaste. Molecules (basel, Switzerland) 26(14):4327

Zaki DY, Hamzawy EMA (2018) In vitro bioactivity of binary nepheline- fluorapatite glass/polymethyl-methacrylate composite. Adv Mater Sci Eng

Publisher's Note